NGS APD tip-tilt : ARGOS commissioning April 2015 run

Gilles Orban de Xivry

June 3, 2015
v 0.1

Contents

1 Introduction

See also report of Feb. 2015 run.

2 Calibration

The geometry with the APD channel numbers is given in Fig. 1 (see also the fiber # to APD# connection in report Feb. 2015).

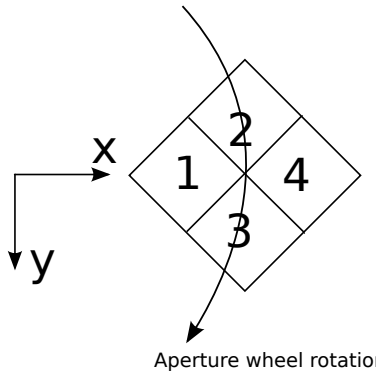

Figure 1: FLAO board axis orientation versus quad-cell. The direction of rotation of the aperture wheel is also indicated. The numbers are the APD channels.

2.1 Dark

Procedure:

- aperture wheel closed & FW2 empty (no QC)
- telescope at zenith
- APD counter integration time 1ms.

We acquire 3×8minutes data, the average is given in Tab. 1. Variation is <1 counts per second.

Table 1: Dark level measured the 27/04/2015.

APD channel	#1	#2	#3	#4
dark [counts/seconds]	229	110	116	110

2.2 Flat

We measure the flat using three different techniques for redundancy, and find out the presence of a secondary spots with the FW1 0.04/99.6 (discussed later in Section 4).

With defocussed internal source. Procedure: Using the internal FLAO light source, FW2 0.04/99.6, and highly defocusing the FLAO board to create a spot of $\sim 4''$(Z = 10mm). With 2 minutes acquisition of $\sim$ 700ph/APD/ms, one measure the relative efficiencies:

$$[91.4, 100, 97.8, 96.6]\%,$$

this is repeated 3× and gives the same results.

With "dome flat". Procedure : dome light on, test of different Z-board position and X and Y. Results is

$$[84, 98, 85, 100]\%.$$

With internal source in focus in each APD Procedure : FW1 0.04/99.6, spot of $\sim 0.5''$(Z = 52.5mm), scan in X and Y to find the maximum in each APD channel. Results is

$$[82, 93, 87, 100]\%$$

Conclusion "Dome flat" and internal source in focus individually in each cell give consitent results, while the defocussed internal source not. As we will see, this is due to a secondary spots with FW1 0.04/99.6.

The final relative efficiencies is given in Tab. 2.

Table 2: Relative efficiencies measured with "dome flat" (percentage wrt to the "best" cell).

APD channel	#1	#2	#3	#4
Relative efficiencies [%]	84	98	85	100

3 Aperture wheel

Procedure : Largely defocus internal source (Z = 10mm), scan of the aperture angle by steps from 0.5 to 2 degrees. The geometry is given in Fig. 1, and explained the sequence of light exposure : APD#2 sees the light first, then #1 and #4 in parallel, and finally APD #4. This is done for all 7 apertures and is shown in Fig. 2 where each APD curve is normalized by its total count.

One can make the following remarks:

- There are two regimes: 1) the chosen aperture is larger than the FoV of a single cell (POS1-POS4), 2) the aperture is smaller (POS5-POS7). In regime 1), the FWHM of the profiles in Fig. 2 gives approx. the FoV of the apertures. While in regime 2), the width of the APD#1 and APD#4 curves give the FoV of one cell (∼6 degree of aperture wheel), and the width of APD#2 and APD#3 gives approx. the size of the aperture.
- Since we know from design - and also measure it in Section 4 - that one cell is approx. $1''$ across, so approx. $1.4''$in diagonal. Thus we have the **conversion from degree of aperture wheel to FoV in arcsec** $\sim 0.2 - 0.23''$**/degree**.

From the curves and those remarks, we derived the FoV of each aperture, see Tab. 3 and Fig. 2.

Table 3: Derivation of the aperture wheel FoV.

Position	aper. wheel rot [deg]	aper. FoV [$''$]
7	∼1.3	∼0.25
6	∼2.5	∼0.5
5	∼5	∼1.0
4	∼7	∼1.5
3	∼10	∼2.0
2	∼12	∼2.5
1	∼16.5	∼3.0

4 Quad-cell scan with FLAO board

We perform different scans of the quad-cell by moving the FLAO board in X and Y, with different FW1 and aperture wheel position and/or different spot focus. The board was moved in the X-direction and the tip-tilt signal was rotated by 45°(software de-rotation) to give a tip.
We do the following measurements, shown in Fig. 3:

a) FW1 0.04/99.6, aperture POS1 (3″)

b) FW1 0.04/99.6, POS6 (∼0.5″)

c) FW1 50/50, POS1.

d) same.

e) FW1 50/50, POS1, spot ∼ 0.5″.

f) FW1 Silver mirror, in focus

g) FW1 Silver mirror, spot ∼ 0.5″.

We can do the following remarks :

- FW1 0.04/99.6 creates a visible secondary spot of approx. half the flux of the primary spot. No secondary spots can be seen for the FW1 50/50 and the Silver mirror.
- from the second plot (b) FW1 0.04/99.6, POS6), we can estimate the **distance between the primary and secondary spots,** $\Delta = 0.915''$.
- Observed in all cases is a central decrease in flux, most likely due to the central lower response of the quad-cell. When the spot is in focus, the spot size is of order of the diffraction limit, ∼13mas, much smaller than the observed dip in the plot. We can estimate an approximate physical size of the dip as ∼0.15 arcsec (from the plots) $\times 0.6mm/'' \times f_{\#} =\sim 1400\mu m$.

5 Interaction matrix computation

Since the co-pointing QC and pyramid was not possible (BCU47 not operational), an alternative for the interaction matrix acquisition had to be found wrt to the procedure applied in Feb. 2015 (see report). This one is described here below. Hence we have two ways of performing the interaction matrix implemented in the ARGOS software.

5.1 Procedure

- scanning the APD by moving the board position in X and Y
- converting the board position to wfs, from X [arcsec] to rms [rms wf surface tip and tilt]:
$$rms = 1/2\ 1/4\ 8.2\ 4.848\ 10^{-6}\ X$$
- map the board coordinates to tip and tilt coordinates.
- having modes and APD slopes (obtained by fit), one can then derived the reconstructor as described in Feb. 2015 report.

5.2 Result

The mapping of coordinates was measured by shifting the FLAO board in X and Y, and recording tip-tilt modes by using the truth sensing[1] on the pyramid with a LUCI de-rotator angle of 0°. One obtains $\theta = 45°$ and the "rotation" matrix (axis flipped and rotation) is

$$\mathbf{Rot} = \begin{bmatrix} -\cos\theta & \sin\theta \\ \sin\theta & \cos\theta \end{bmatrix} \quad (1)$$

The calculated reconstructor was

$$\mathbf{R} = \begin{bmatrix} -6.696e-11 & 2.995e-12 \\ 1.694e-12 & -6.54e-11 \end{bmatrix} \quad (2)$$

valid for a zero-angle of 0°, as parameter in the Bonn unit. Hence, only the LUCI rotator angle has to be updated at the parameter "rotation angle" of the Bonn unit (as already implemented). Note as well, that this is in better agreement to the simple theoretical calculation than previously found (see report Feb.2015).

Coordinates & K-mirror vs. LUCI rotator angle Conversion in degree between LUCI rotator angle and Pyramid K-mirror angle depends on the FLAO binning and is :

$$\alpha_K = C - \frac{\alpha_{LUCI}}{2}$$

with

$$\begin{aligned} C &= 271.15 \quad \text{Bin1} \\ &= 303.85 \quad \text{Bin2} \\ &= 270.35 \quad \text{Bin3, Bin4} \end{aligned}$$

[1] *N.B.; truth sensing does not work in bin1, even if it is returning values...*

6 Conclusion

- dark & flat have been measured, and both are good. (Note however that the fiber head coupled to APD#1 is still damaged and thus very fragile).
- the different apertures FoV have been measured, and the software wheel positions are well centered.
- Because of a secondary spot with $\Delta \sim 0.9''$, the FW1 0.04/99.6 is not optimum for closed-loop operation (one performs the measurement on the two stars barycenter instead on a single star). This is OK since it is not a common configuration (except to perform tip-tilt on very bright stars).
- We are missing a filter of type 90/10 on FW1 (90% to QC, 10% to pyramid). To perform tip-tilt on faint star and truth sensing in parallel. The only usable filter on sky for proper closed-loop is thus at the moment the FW1 50/50.
- Tip-tilt reconstructor acquisition is working well. It relies - in both cases - on the Pyramid truth sensing.

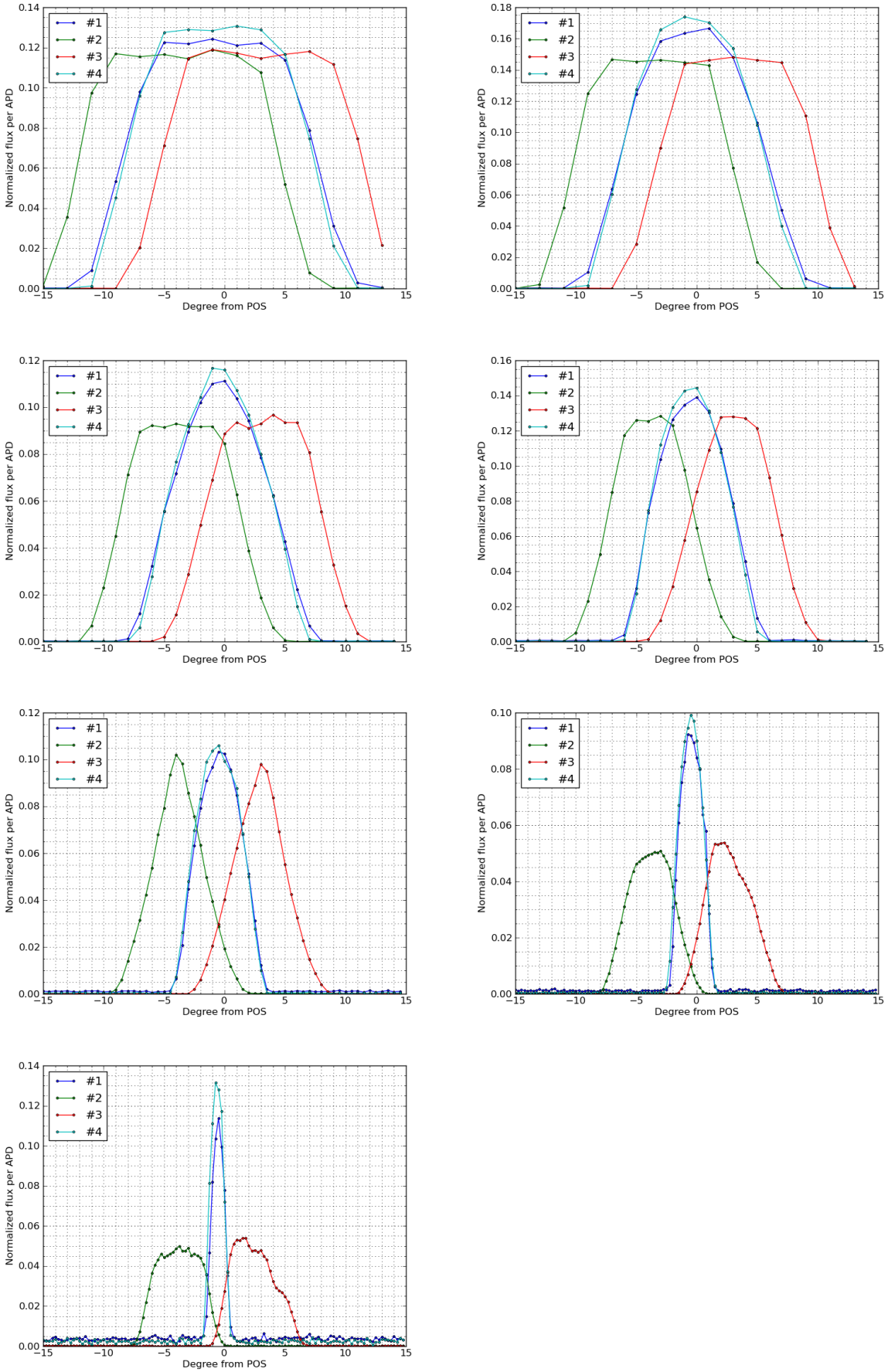

Figure 2: From top left to bottom: POS1 to POS7. 1st row : (left) POS1 3″, (right) POS2 2.5″. And so on, see also Tab. 3

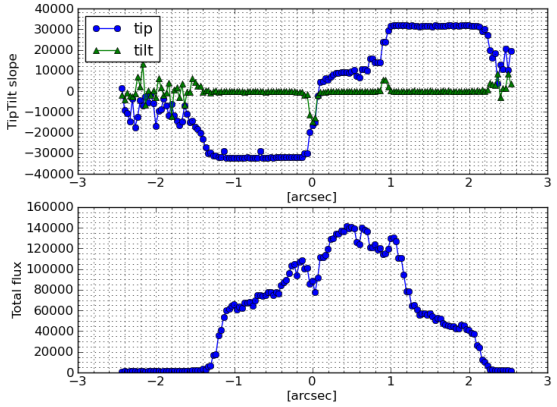

(a) FW1 0.04/99.6, aper. POS1 (3″)

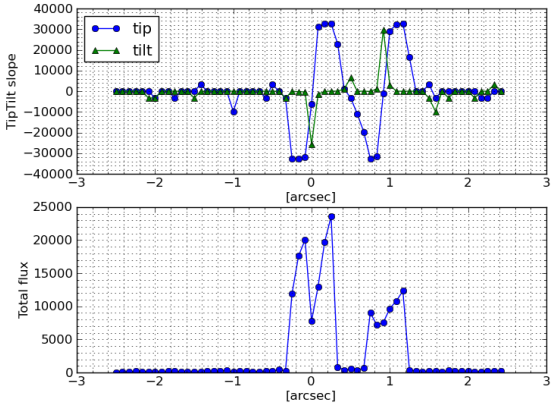

(b) FW1 0.04/99.6, aper. POS6=0.5″

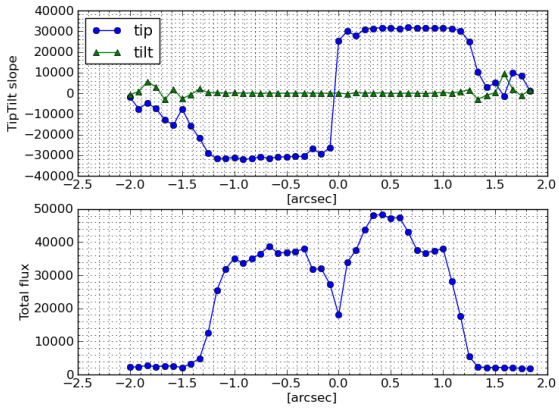

(c) FW1 50/50, POS1

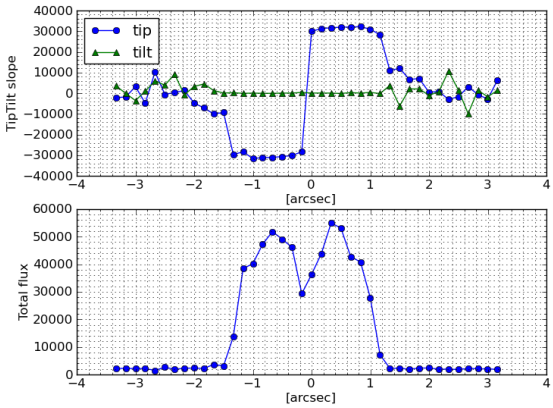

(d) FW1 50/50 (same, different scale)

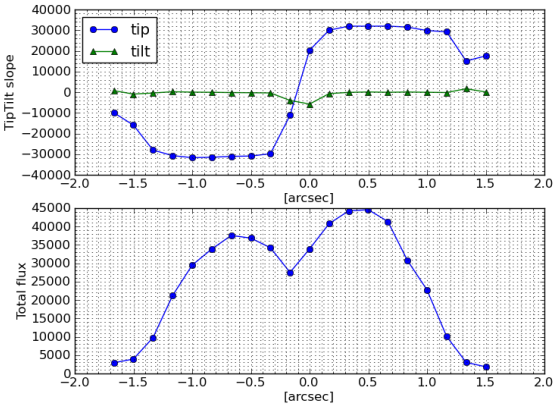

(e) FW1 50/50, 0.5″spot, aper POS1

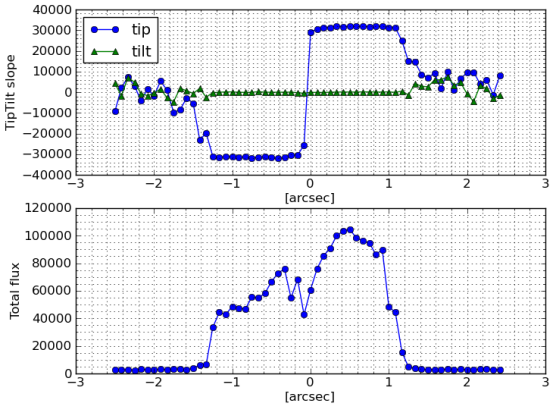

(f) FW1 silver mirror

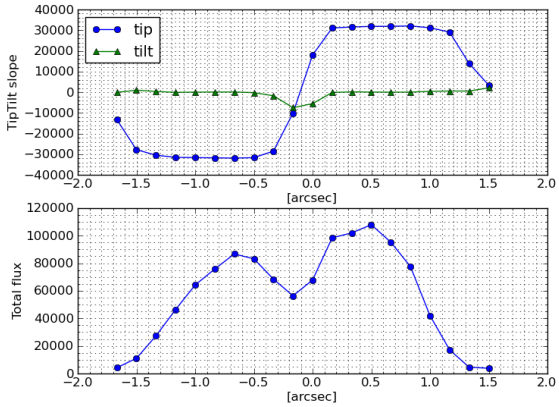

(g) FW1 silver mirror, defocus 0.5″spot

Figure 3: Tip-tilt slopes and total flux with different filter in FW1, apertures and/or spots sizes.